

Chapter 1

Introduction

This document is a report on the analysis of the data from Phase 1 of the calibration of the Advanced X-ray Astrophysics Facility (AXAF), which occurred between 1996 December 20 and 1997 February 11 at the X-Ray Calibration Facility (XRCF) at Marshall Space Flight Center (MSFC) in Huntsville, Alabama. The analysis of these data is still ongoing; this document is an update to Jerius (1997).

Because there isn't time in the lifetimes of the members of the team to completely calibrate or characterize every facet of the HRMA, the measurements are augmented by a highly detailed mechanical and optical ray-trace model of the HRMA. The XRCF measurements are used to refine and correct the *ab initio* and semi-empirical components which make it up. Chapter 10 provides more details.

During this test program, we ran a total of 1376 logical tests, each identified by an alphanumeric "TRW ID," assigned according to a scheme negotiated between the prime contractor, TRW, and the AXAF science community. Of these, 982 tests were done without transmission gratings, mostly for the calibration of the High Resolution Mirror Assembly (HRMA), or of the facility (such as background, beam uniformity, alignment to facility axis, etc.). The HRMA X-ray Detection System (HXDS) obtained a total of 5225 different run identifiers (runid's), which include 293,144 individual pulse-height spectra and 1486 High Speed Imager (HSI) images.

The HRMA-only tests will be described in some detail in this document. In Phase 2 of the XRCF test program, science instruments and their stand-ins were used at the focal point of the telescope. Those data are not presented here, though in many cases they bear on the same questions as the Phase 1 data.

TBR: Several puzzles remain to be solved. Most notable among these is the discrepancy in the effective area, discussed in Chapter ???. Raytrace simulations predict an effective area significantly higher than that which is measured by two different techniques. In most cases this discrepancy amounts to $\sim 8-10\%$, though for mirror pair 1 near its high energy cutoff, the discrepancy is even larger.

1.1 The Facility and Experimental Setup

The test setup is described in detail elsewhere (for example, in SAO (1997)), but a brief description is in order here. A set of X-ray sources is available in Building 600. These include the Electron Impact Point Source (EIPS), a Penning source, and two monochrometers which select X-ray photons emitted by rotating anode sources. These are the Double Crystal Monochromer

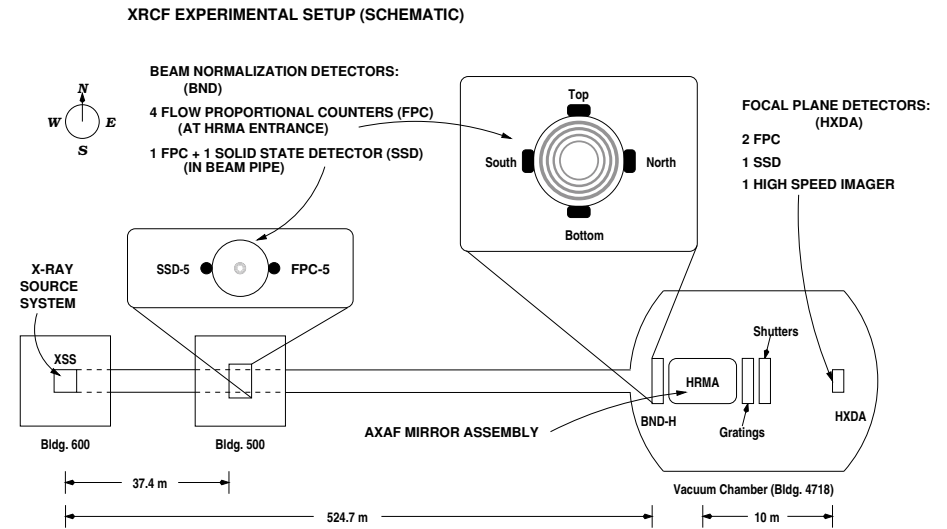


Figure 1.1: Schematic of XRCF

(DCM), and the High Resolution Erect Field Spectrometer (HIREFS).

Figure 1.1 shows the physical layout of the XRCF. Connecting Building 600 to the main instrument chamber in building 4718 at MSFC is an evacuated guide tube over 500 meters long. Approximately 38 meters down the guide tube in Building 500, but off to one side of the beam to avoid occulting it, are two beam normalization detectors (BND) known as the BND-500. These are a Flow Proportional Counter (FPC), *fpc_5*, and a solid state detector (SSD), *ssd_5*. The *fpc_5* detector can be moved about in the beam by a pair of translation stage motors, to map the beam and test it for uniformity. The *fpc_5* is closer to the source than the *ssd_5*. Both of the BND-500 detectors have selectable apertures.

The main instrument chamber contains a variety of equipment, including the HRMA, a set of BNDs surrounding the entrance to the HRMA, and the focal plane instrumentation, the HRMA X-ray Detector Assembly (HXDA). It also contains the flight Objective Transmission Gratings, a set of quadrant shutters (which allow each quadrant of each of the 4 constituent optic pairs of the HRMA to be exposed independently), the HRMA contamination covers, and various motors and other hardware to support operations.

The BND assembly at the HRMA entrance is known as the BND-H (Beam Normalization Detectors at the HRMA). It consists of four nearly identical flow proportional counters, whose nominal stations are adjacent to the north, bottom, south, and top quadrants of the outermost HRMA mirror shell. They are known, respectively, as *fpc_hn*, *fpc_hb*, *fpc_hs*, and *fpc_ht*. The *fpc_hn* detector can be moved around in front of the HRMA entrance to map the X-ray beam as it enters the HRMA. It is physically located a small distance closer to the source than the other three BND-H detectors. It can be used either with a 36 mm diameter circular aperture, in the open configuration.

The HXDA assembly at the HRMA focal point consists of two Flow Proportional Counters (FPC), one Solid State Detector (SSD), and a microchannel plate camera known as the High Speed

Imager (HSI). These detectors are known respectively as `fpc.x1`, `fpc.x2`, `ssd.x`, and HSI. The two FPCs are a redundant pair. Except for an early aliveness check, all of the FPC tests actually performed were done with `fpc.x2`.

All of the HXDA detectors are mounted on a stack of translation stages which allow them to be placed anywhere in three dimensions in the vicinity of the telescope focus, with an accuracy of about 2 μm . They also allow the apertures for the FPCs and SSD to be selected. FPC aperture sizes range from 3 μm to 35 mm diameters; apertures smaller than 7.5 μm were rarely used. Computations based on the positions of these stages are outlined in Chapter 8.

The BNDs are exposed simultaneously with the focal plane detectors. Focal plane count rates are normalized by the photon flux density at the BNDs, leading to *aperture-relative* effective areas, in units of cm^2 . These are aperture-relative since the focal plane detectors have finite size. Chapter 9 and Chapter 12 go into more detail about the reduction efforts.

A great many facility physical dimensions are required to fully characterize the experiment for data reduction purposes. Chapter A lists a few of the most important dimensions, and the values they were assumed to have.

1.2 The Measurements

The objective of the test program is to validate a high-fidelity ray trace model of the HRMA, which includes a wide variety of information about the physical and engineering properties of the mirror assembly, including, for example, the effects of gravity, offloader stresses, epoxy shrinkage, surface deformations and roughness, rigid body position of the optical elements, etc. After the model is revised and validated by comparing its predictions to the XRCF data, it can then be used with considerable confidence to predict the performance of the mirrors on orbit.

Accordingly, the test program included a variety of experiments. These include measurements of encircled energy fractions *vs.* aperture size and measurements of effective area at various energies (see Figure 1.2 for a graphical summary of these tests); aperture scans of the wings of the point spread function (see Figure 1.3); measurements of the microroughness of the ends of the mirrors through encircled energy tests with the mirrors tilted to approximate the incident angles of photons from a point source at infinity (see Figure 1.4); 1- and 2-dimensional aperture scans of the point spread function (see Figure 1.5 and Chapter ??); images of the point spread function (both the inner core of the image, and with that occulted, the outer core) and images taken to constrain the internal alignment of the HRMA optics (see Figures 1.6 and 1.7); images and aperture scans at the ring focus position; various attempts to detect molecular contamination (if any); measurements of the alignment of the mirror to the facility optical axis; shutter focus measurements; and various kinds of grating tests.

Brief descriptions of the measurements follow; many of them are described more fully, including the results and the analysis done to date, in the ensuing chapters.

Focus and Tilt

The focal position and the intra-shell tilt of the mirrors can be determined by exposing, in turn, each quadrant of a mirror (or mirrors) with the quadrant shutters, and measuring the centroid of the resultant images. The offsets of the centroids allow calculation of the focus and tilts. With the HSI, this is an actual image, but with the FPC or SSD we make a 2 dimensional raster scan with a small pinhole. These measurements were typically made for each shell individually. (See Chapters 26 and 28).

Encircled Energy/Effective Area

Each of a series of pinholes is carefully centered on the image centroid. The effective area

as seen by each pinhole is given by

$$A_{\text{eff, pinhole}} = A_{\text{BND}} \times \frac{R_{\text{pinhole}}}{R_{\text{BND}}}$$

where A_{BND} is the open area of the BND. R_{pinhole} is the count rate through the pinhole, and R_{BND} is the count rate seen by the BND. The pinholes typically cover 0.1'' to 6' radius around the image center. Effective area measurements are a special case of the encircled energy for the largest available pinhole. (See Chapters 16 and 12.)

Point Response Function

The PRF of the mirrors was measured in two regimes. The inner core was sampled with one and two dimensional pinhole scans centered about the image centroid. The outer core was measured with the HSI by placing the inner core on specially designed masks. A one dimensional scan through the center gives the Full Width at Half Maximum measurement. Two dimensional scans can be deconvolved for ground effects to deduce the properties of the mirror in orbit. (See Chapters 19 and ??.)

Wing Scan

The far outer wings of the PRF are measured via a one-dimensional scan with a relatively large pinhole. These measurements are generally made using one quadrant of one mirror; the direction of the scan was in the plane of the incident and reflected ray at the midpoint of the quadrant. Typical scans are 20'' to 35' from the image center. During many scans the HRMA was tilted so that the grazing angle of the photons from the XSS with respect to the mirror would be more similar to that on orbit. (See Chapters 14 and 15.)

Ring Focus

The ring focus describes a position on the optical axis of the HRMA where spherical aberration due to a finite-distance source causes the rays from the front and back of the mirrors to cross, giving a minimum thickness ring which is ideal for analyzing 1g mechanical effects on the ground calibration. HSI images were taken at the ring focus position, which for the HRMA is 65.2 mm in front of the finite distance focal point. (See Chapter 18.)

Background

Runs were made with the gate valve from the source chamber closed, so that there were no X-rays from the source. Setup of the detectors was identical to a subsequent series of measurements with a given X-ray source.

Beam Uniformity

Two dimensional scans made with the BNDs at the HRMA and at at Bldg. 500. These scans approximated coverage of the region of space occupied by the HRMA, and by the fixed bnd detectors. (See Chapter 24.)

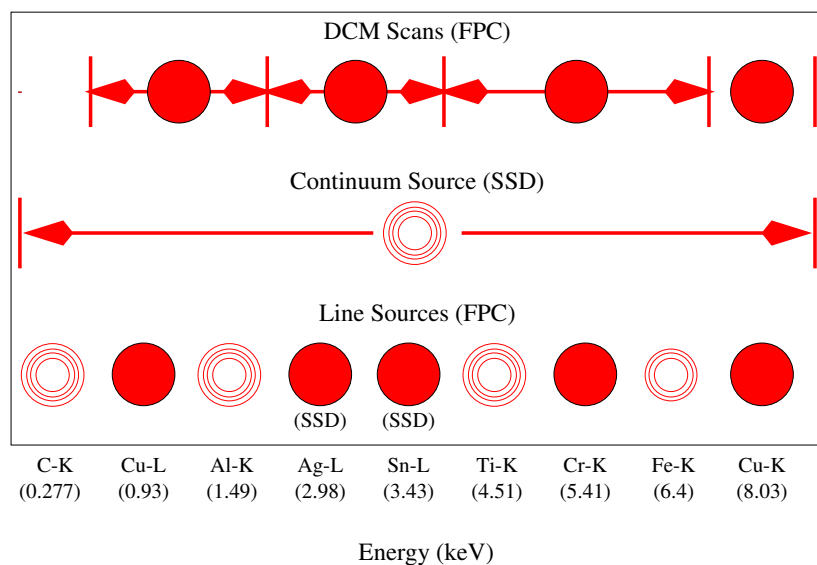


Figure 1.2: The on-axis encircled energy/effective area tests were performed using 3 complementary methods: 1) Line sources with the FPC (bottom row), a continuum source (i.e., the carbon anode run at a high voltage) with the SSD (middle row), and the DCM with the FPC (top row). Filled circles indicate tests that were done with the full HRMA, while open circles indicate tests that were done with single shells (e.g., 4 concentric circles indicate that the test was done for each shell separately).

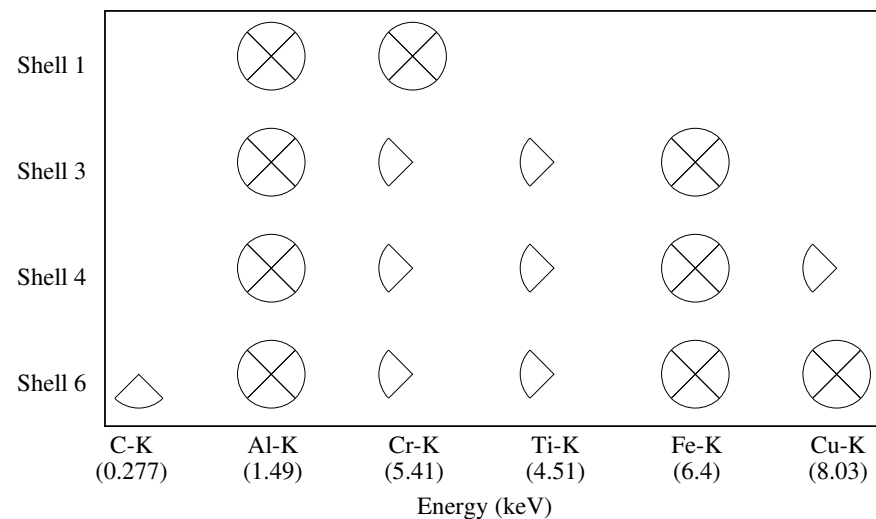


Figure 1.3: All wing scans were performed with only one quadrant of one shell open. This figure shows the wing scan measurements that were performed during Phase 1 as a function of energy, shell, and quadrant. The south quadrant is on the left and the north quadrant is on the right.

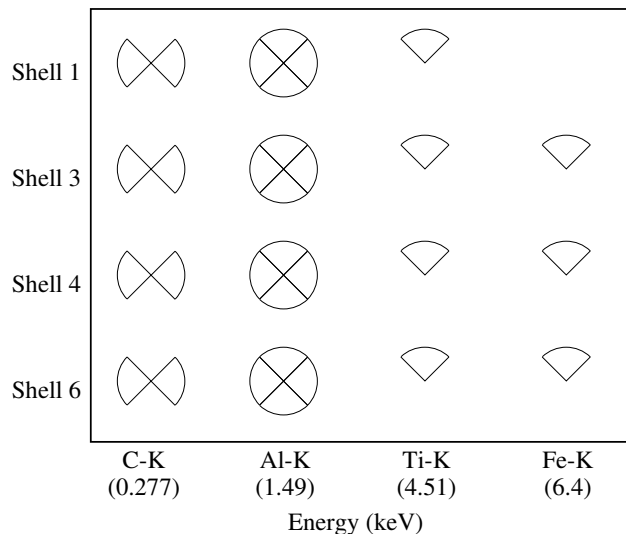


Figure 1.4: Mirror ends survey measurements completed during Phase 1 as a function of energy, shell, and quadrant. The south quadrant is on the left and the north quadrant is on the right.

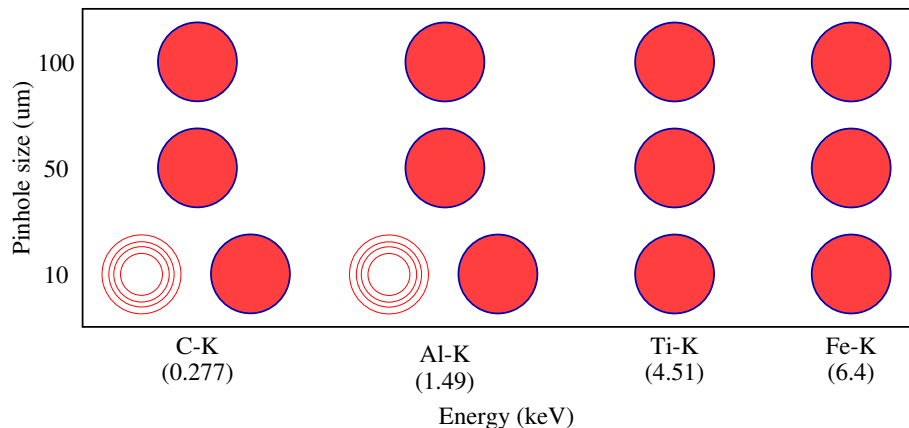


Figure 1.5: 2-D pinhole scans performed during Phase 1 as a function of energy and pinhole diameter. Filled circles indicate tests that were done with the full HRMA, while open circles indicate tests that were done with single shells.

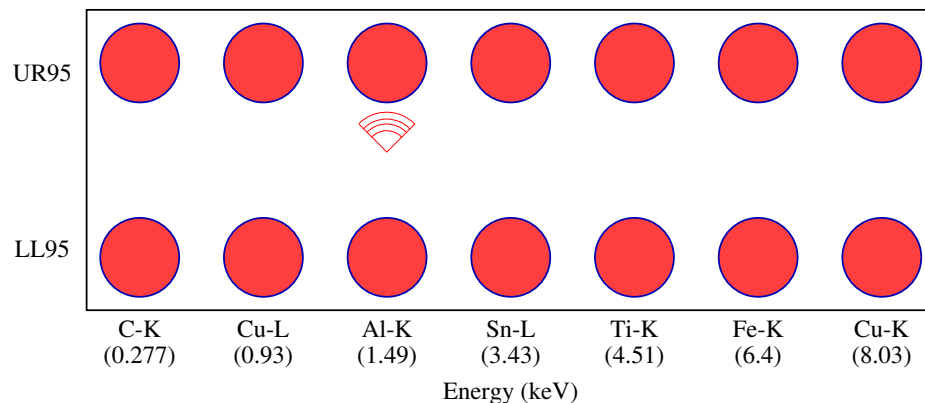


Figure 1.6: PSF Outer core measurements performed during Phase 1 with the HSI. The HSI has two cusps which can block out the centroid of the image. One is on the upper right of the detector (UR95) and one is on the lower left (LL95). The pie slice at Al-Ka indicates images that were obtained with only the top shutter open for individual shells.

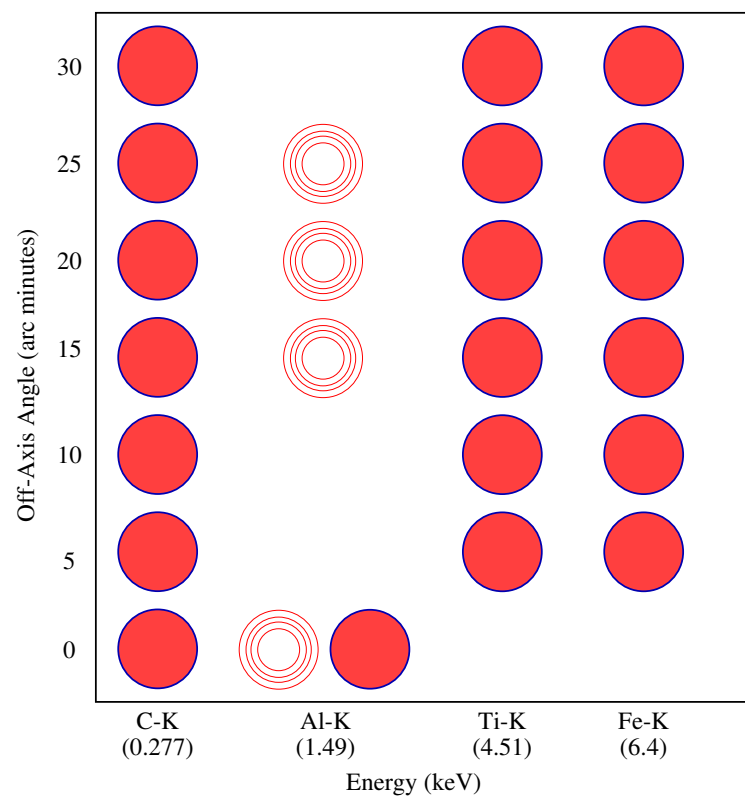


Figure 1.7: HSI images obtained during Phase 1 as a function of energy and angle off-axis. Filled circles indicate tests that were done with the full HRMA, while open circles indicate tests that were done with single shells.